

Editorial Manager(tm) for Geology
Manuscript Draft

Manuscript Number: G30720R1

Title: Basaltic scoria textures from a zoned conduit as precursors to violent Strombolian activity

Short Title: Basaltic scoria textures as precursors to violent Strombolian activity

Article Type: Article

Keywords: Violent Strombolian; mingling; conduit dynamics; precursors; Garrotxa

Corresponding Author: Dr Jacopo Taddeucci,

Corresponding Author's Institution: Istituto Nazionale di Geofisica e Vulcanologia

First Author: Corrado Cimarelli

Order of Authors: Corrado Cimarelli; Federico Di Traglia; Jacopo Taddeucci

Manuscript Region of Origin: ITALY

Abstract: Pyroclast textures document volcanic conduit processes and may be key to hazard forecasting. Here we show that the relative abundance of mingled, variably crystallized domains in pyroclasts from scoria cone eruptions provide a record of magma ascent velocity and can be used to predict the onset of violent Strombolian activity. Scoria clasts from the Croscat Complex Scoria Cone (Spain) ubiquitously show mm to cm-sized, microlite-rich domains (MRD) intermingled with volumetrically-dominant, microlite-poor ones (MPD). Glass and bulk composition show that MRDs formed by microlite crystallization of MPDs, the former residing longer in a relatively cooler, degassed zone lining the conduit walls, the latter traveling faster in the central, hotter streamline. MPD and MRD magmas intermingled along the interface between the two velocity zones. The proportion of MPD and MRD in different tephra layers reflects the extent of the fast- and slow-flowing zones, thus reflecting the ascent velocity profile of magma during the different phases. At Croscat, the MPD/MRD volume ratio increased rapidly during the early Strombolian activity, peaked around the Strombolian to violent Strombolian shift, and then decreased smoothly irrespective of shifts in eruptive style. We suggest that magma ascent velocity escalated during the Strombolian phase due to the buoyant push of the underlying, volatile-rich magma that was about to drive the following violent Strombolian activity. Monitoring the MPD/MRD ratio of tephra during ongoing scoria cone eruptions may reveal changes in magma flow conditions and could forecast the onset of hazardous violent Strombolian activity.

Response to Reviewers: Dear Editor of Geology,

The present cover letter accompanies the revision of the manuscript "Basaltic scoria textures from a zoned conduit as precursors to violent Strombolian activity" by C. Cimarelli, F. Di Traglia and J. Taddeucci (Ref.: Ms. No. G30120).

The manuscript has been integrated according to all the minor revisions of both reviewers. All of them were constructive and led to significant improvements of the final version of the manuscript.

All suggestions and comments of reviewer #1 have been fully accepted and incorporated in the present version of the manuscript. The reviewer #2 did not suggest any further change in the manuscript and

we wish to thank her for the encouraging suggestions and the detailed review on the previous version of the manuscript.

We also incorporated the few comments of the managing editor and, in particular, the text format used in the figure has been corrected according to the Geology format (see correction of capital letters in all the figures). Also the references cited in the text have been updated according to those reported in the reference list.

Please find below a synthetic list of the reviewer #1 comments to the previous version and the changes we accordingly introduced in the new manuscript.

Reviewer #1

1) Localization of the crystallization and mingling event.

We added a new sentence in lines 140-145, fully accepting the reviewer's view.

2) Timescales of eruption and analytical procedures.

Again, we accepted the suggestion and included a new sentence in lines 169-171.

3) Revision of Figure 3.

Following the recommendation by Reviewer #1, we modified the Fig. 3 omitting the estimated duration scale of the eruption that was previously indicated on the right hand side of the diagram. The information on eruption duration is now included in the caption.

Sincerely yours,

Corrado Cimarelli, Federico Di Traglia, Jacopo Taddeucci.

Supplemental file

[**Click here to download Supplemental file: Appendix_Cimarelli^{etal}_resub.doc**](#)

Cover letter

[**Click here to download Cover letter: Cover_letter_CimarellietaL.doc**](#)

Publisher: GSA

Journal: GEOL: Geology

Article ID: G30720

1 Basaltic scoria textures from a zoned conduit as precursors to 2 violent Strombolian activity

3 **C. Cimarelli¹, F. Di Traglia², and J. Taddeucci³**

4 ¹Dip. Scienze Geologiche, Università Roma Tre, L.go S.L. Murialdo 1, 00146 Rome, Italy

5 ²Dip. Scienze della Terra, Università di Pisa, Via S. Maria 53, 56126 Pisa, Italy

6 ³Istituto Nazionale di Geofisica e Vulcanologia, Via di Vigna Murata 605, 00143 Rome, Italy

7 ABSTRACT

8 Pyroclast textures document volcanic conduit processes and may be key to hazard
9 forecasting. Here we show that the relative abundance of mingled, variably crystallized domains in
10 pyroclasts from scoria cone eruptions provide a record of magma ascent velocity and can be used to
11 predict the onset of violent Strombolian activity. Scoria clasts from the Croscat Complex Scoria
12 Cone (Spain) ubiquitously show µm- to cm-sized, microlite-rich domains (MRD) intermingled with
13 volumetrically-dominant, microlite-poor ones (MPD). Glass and bulk composition show that MRDs
14 formed by microlite crystallization of MPDs, the former residing longer in a relatively cooler,
15 degassed zone lining the conduit walls, the latter traveling faster in the central, hotter streamline.
16 MPD and MRD magmas intermingled along the interface between the two velocity zones. The
17 proportion of MPD and MRD in different tephra layers reflects the extent of the fast- and slow-
18 flowing zones, thus reflecting the ascent velocity profile of magma during the different phases. At
19 Croscat, the MPD/MRD volume ratio increased rapidly during the early Strombolian activity,
20 peaked around the Strombolian to violent Strombolian shift, and then decreased smoothly
21 irrespective of shifts in eruptive style. We suggest that magma ascent velocity escalated during the
22 Strombolian phase due to the buoyant push of the underlying, volatile-rich magma that was about to
23 drive the following violent Strombolian activity. Monitoring the MPD/MRD ratio of tephra during
24 ongoing scoria cone eruptions may reveal changes in magma flow conditions and could forecast the
25 onset of hazardous violent Strombolian activity.

26 **INTRODUCTION**

27 Basaltic volcanism, ranging in intensity from effusive to violent explosive, is the prevailing
28 volcanic activity on Earth. Of the variety of explosive styles shown by basaltic eruptions, ranging
29 from Strombolian to Plinian intensities (e.g., Vergniolle and Mangan, 2000), violent Strombolian
30 activity (MacDonald, 1972) is currently under reappraisal. An increasing number of past eruptive
31 successions are being reclassified as violent Strombolian (Arrighi et al., 2001; Valentine et al.,
32 2005, 2007; Di Traglia et al., 2009), as are recently observed events, including the 1943–52 type-
33 eruption of Paricutin (MacDonald, 1972; Luhr and Simkin, 1993; Pioli et al., 2008), the 1995 Cerro
34 Negro eruption (Hill et al., 1998), and the 2002–2003 eruption of Mt. Etna (Andronico et al., 2009).
35 In all the above geological and historical cases, violent Strombolian activity represents the peak-
36 intensity phase of months- to years-lasting eruptions, punctuating other lower-intensity explosive
37 and effusive phases and producing eruptive plumes several kilometers in height with occasional
38 small-scale column collapses, posing severe threats to inhabited areas (Houghton et al., 2006;
39 Andronico et al., 2009).

40 Similar to other high-intensity explosive phases (Rosi et al., 2006; Sable et al., 2006), the
41 onset of violent Strombolian activity during complex mafic eruptions is inferred to be related to the
42 arrival of volatile-rich magma batches (Andronico et al., 2009; Pioli et al., 2008) and/or to changes
43 in the rheological properties of magma, as related to microlite crystallization within the conduit
44 (Valentine et al., 2005; Andronico et al., 2009), with conduit geometry and branching as additional
45 controlling factors (Keating et al., 2008; Pioli et al., 2009). Violent Strombolian phases require
46 relatively high magma mass flow and ascent velocities (Parfitt, 2004) as well as efficient magma
47 fragmentation, as testified by grain-size and morphology (Andronico et al., 2009; Valentine and
48 Gregg, 2008). Vesicularity of violent Strombolian scoriae, ranging between 50%–70% versus 30%–
49 80% in Strombolian scoriae (Polacci et al., 2008; Pioli et al., 2008; Di Traglia et al., 2009), and
50 bubble number density (BND) values intermediate between Hawaiian and Plinian products, suggest
51 relatively fast decompression of gas-rich magmas compared to lower intensity explosive eruptions

52 (Houghton and Gonnermann, 2008; Di Traglia et al., 2009). Pyroclasts from violent Strombolian
53 products are typically porphyritic with both glassy and cryptocrystalline groundmasses (e.g., Pioli et
54 al., 2008), interpreted to be the result of different degrees of magma crystallization within different
55 zones of the conduit (Taddeucci et al., 2004). Large microlite contents are expected to change the
56 rheological behavior of basaltic magma both during conduit flow (Lejeune and Richet, 1995) and at
57 fragmentation (Taddeucci et al., 2007), ultimately controlling the eruptive style.

58 In the present paper, we use textural features of mingled scoriae from the basaltic eruption
59 of the Holocene Croscat Complex Scoria Cone (Spain) to shed light on conduit flow conditions
60 during the transition from Strombolian to violent Strombolian activity, potentially offering a means
61 to forecast the onset of hazardous violent Strombolian events during ongoing eruptions.

62 **The Croscat Complex Scoria Cone**

63 The Croscat Complex Scoria Cone (CCSC) is the youngest volcano of the Garrotxa
64 Volcanic Field and of the whole Iberian Peninsula (11 ka; Guérin et al., 1985), and its volcanic
65 succession provides an excellent example of highly variable activity within a single mafic eruption.
66 The eruption started with fissural Hawaiian activity (LQU; Fig. 1), shifted to Strombolian
67 explosions from a central vent (UQU), and then magma interaction with a shallow aquifer system
68 promoted the first phreatomagmatic phase (CCU). The arrival of a relatively gas-rich, more
69 primitive magma (as testified by trace element variations; Di Traglia et al., 2009), possibly
70 decompressed by the preceding phreatomagmatic activity, drove three violent Strombolian phases,
71 producing widespread tephra blankets (lower, middle and upper CMU). Subsequently, the activity
72 shifted into a second, larger phreatomagmatic phase (CBU). The eruption ended with the emission
73 of a lava flow (CXL) and consequent breaching of the western side of the cone. BND values in
74 CCSC products reveal that ascent rate initially increased at the end of the Strombolian phase, then
75 subsequently became constant during the violent Strombolian phase and finally decreased until the
76 end of the eruption. Stratigraphy and erupted volumes suggest that eruption duration was in the
77 short to average range of scoria cone eruptions (Di Traglia et al., 2009), i.e., several months.

78 **Texture and Composition of Mingled Scoria Clasts**

79 From the best exposed proximal section of the cone we collected 14 samples representative
80 of all tephra units and analyzed thin sections of scoria lapilli under binocular, petrographic, and
81 Field-Emission Scanning Electron Microscope (FE-SEM) (see Methodological Appendix in the
82 GSA Data Repository¹). Scoriae from all stratigraphic units, irrespectively of the eruptive
83 mechanism, show intermingling of two distinct textural domains that we term microlite-poor
84 (MPD) and microlite-rich domains (MRD), respectively (Fig. 2). MPDs are made up of
85 sideromelane glass (pale yellow to brown in thin section) with abundant spherical vesicles down to
86 a few μm in diameter, and include up to 1–2 vol.% of 1–50 μm -sized microlites of plagioclase (Pl),
87 clinopyroxene (Cpx), oxides (Ox), and occasional olivine (Ol). With respect to MPDs, MRDs
88 (dark-opaque and tachylite-like in thin section) are less vesicular, include larger and more irregular
89 vesicles, and contain a significantly larger fraction (15–43 vol.%) of the same microlites. Microlites
90 are mostly euhedral, with evidence of zonation in the Cpx, subordinate skeletal habits occurring in
91 Ol and Plg. Phenocrysts of Ol and Cpx equally occur in both domains. The two domains are
92 commonly found intermingled in the same scoria clast, with individual domains ranging in size
93 from \sim 30 μm to the size of the whole clast. Domain boundaries, defined by a sharp (mostly $<1 \mu\text{m}$ -
94 thick) transition of glass composition (highlighted by the gray tone of BSE images), are mostly
95 convoluted and show fluidal re-orientation of prolate microlites in MRDs, independent of clast or
96 vesicle preferential orientations.

97 Electron Microprobe (EMPA) and FE-SEM spot and bulk chemical analyses (see Appendix)
98 of MPDs and MRDs show that interstitial glasses in MRDs follow a clear differentiation trend, with
99 the MPD counterparts representing the most primitive extremity. Notably, MRDs bulk composition
100 is comparable (within analytical error) to that of adjoined MPD glass (Fig. 2).

101 In order to obtain a fast and accurate measure of the relative abundance of MPDs and MRDs
102 up-section in the Croscat deposits, we classified 2–4 mm particles as “MR” or “MP” on the basis of
103 their prevailing groundmass texture under petrographic microscope (see Appendix). The results

104 (Fig. 3) show a smooth trend, with a rapid increase of the MPD/MRD vol. ratio within the
105 Strombolian deposit, a peak around the transition to violent Strombolian ones, and a gradual
106 decrease up-section, with no major changes corresponding to shifts in eruptive style (e.g., the
107 magmatic-phreatomagmatic transition).

108 **INTERPRETATION AND CONCLUSIONS**

109 **Conduit Flow Dynamics During Complex Explosive Basaltic Eruptions**

110 The clear differentiation trend of interstitial MRD glasses, the chemical homogeneity of
111 MRD bulk and MPD interstitial glass compositions, and the occurrence of an identical phenocrysts
112 assemblage, all together reveal that MPDs and MRDs represent portions of the same magma that
113 experienced different degrees of microlite crystallization. Microlite abundance and vesicle
114 abundance and shape (e.g., Mangan and Cashman, 1996) suggest a longer conduit residence time of
115 MRDs with respect to MPDs. Horizontal velocity gradients within conduits were already postulated
116 to generate magma zoning during mafic explosive activity with respect to both vesicularity (Lautze
117 and Houghton, 2005) and microlite crystallization patterns (Taddeucci et al., 2004). We hypothesize
118 that MRDs resided longer in a relatively cooler zone lining the conduit margins, where degassing
119 was also favored, while MPDs traveled faster in a hotter environment along the central streamline
120 of the conduit. Groundmass textures thus would outline horizontal velocity gradients, averaged over
121 the length of the MRD-forming zone of the conduit. We note that, in the CCSC case, such gradients
122 persisted throughout the eruption.

123 The mingling of MPDs and MRDs may illuminate flow dynamics of the velocity-zoned
124 CCSC conduit. In our scenario, the two domains mingle at the boundary between the two zones of
125 the conduit with different ascent velocities. This boundary, given the lack of domains texturally and
126 compositionally intermediate between MPD and MRD, was relatively sharp and hosted, at least
127 locally, turbulent flow conditions, as testified by the convoluted morphology of the domains.
128 Physical mingling was driven by the velocity gradient occurring between the two domains and

129 controlled by their strong rheological contrast, as related to the high solid fraction of MRDs (Fig.
130 4).

131 The MPD/MRD volume ratio of erupted products reflects the extent of the two domains at
132 fragmentation as related to variable magma flow conditions, and is expected to be mainly controlled
133 by conduit geometry (specifically the volume/surface ratio) and magma ascent velocity. In the
134 CCSC case, the dispersal and country-rock content of erupted products, which are proxies to
135 changes in conduit size or shape, do not correlate with MPD/MRD. Conversely, MPD/MRD
136 broadly correlates positively with another, independent measure of magma ascent velocity, i.e.,
137 BND (Toramaru, 2006; Di Traglia et al., 2009), supporting the notion that velocity changes during
138 the eruption caused the observed up-section variations in MPD/MRD, which, in this case, acts as a
139 magma flow speedometer.

140 The smooth variation of MPD/MRD in the eruption products points out equally smooth
141 changes in magma flow conditions over the time scale represented by each of our samples, likely
142 days to weeks. The fact that MPD/MRD varied smoothly irrespective of abrupt changes in eruptive
143 style implies that the formation and mingling of the two domains occurred below the fragmentation
144 zone, at a level deep enough not to be affected by external factors (e.g., contact with external water)
145 but shallow enough to preserve the domains from mixing.

146 **Strombolian to Violent Strombolian Transition and Eruption Monitoring Implications**

147 The observed MPD/MRD trend indicates a rapid increase of magma ascent velocity during
148 the Strombolian activity, peak velocity during the violent Strombolian phase, and a gradual velocity
149 decrease until the end of the eruption.

150 Focusing on the Strombolian to violent Strombolian transition, we note that, despite the
151 large difference in their intensity and style, peak magma ascent velocity, as recorded by
152 MPD/MRD, was similar during the two phases, and also during the intervening phreatomagmatic
153 activity. Violent Strombolian activity was driven by a batch of magma slightly less evolved and
154 more volatile-rich in comparison to that driving the earlier Strombolian one (Di Traglia et al.,

155 2009). This volatile-rich magma exerted a strong buoyancy lift on the overlying, relatively gas-poor
156 magma filling the conduit. The increasing magma ascent velocity during Strombolian activity could
157 reflect a combination of two factors: 1) the increasing buoyancy of the gas-charged magma as it
158 ascended, magmastic pressure decreased, and bubbles expanded; and 2) the progressive reduction
159 of viscous resistance as the gas-poor magma column was evacuated, also favored by the decrease in
160 the thickness of the microlite-rich, more viscous conduit lining (see Lautze and Houghton, 2007).
161 Even if accelerated to similar ascent velocities, the overlying magma drove moderate Strombolian
162 activity due to its relatively low volatile content, in contrast with the underlying, volatile-rich
163 magma that, reaching the surface, fueled violent Strombolian activity (Fig. 4).

164 Mingled textures occur in other violent Strombolian eruption products (Andronico et al.,
165 2009; Pioli et al., 2008), suggesting that the processes active during the CCSC eruption may be
166 common in complex basaltic explosive eruptions. Textural monitoring of pyroclasts during ongoing
167 basaltic eruptions already proved to be capable of identifying, and to some extent anticipate,
168 increasing intensity of basaltic explosive activity (Taddeucci et al., 2002). The CCSC case provides
169 an interpretative framework for previous cases. Moreover, our methodology allows MPD/MRD to
170 be measured within a few hours after sample collection (see Appendix) and may be included in
171 textural monitoring of basaltic volcanoes. Daily MPD/MRD measures could reveal fluctuations in
172 the magma ascent rate of ongoing eruptions, eventually heralding the arrival of gas-charged magma
173 and the onset of more violent activity.

174 **ACKNOWLEDGMENTS**

175 We thank D. De Rita, G. Ventura and E. Del Bello for thoughtful discussions, and A.
176 Clark, G. Valentine, M. Hort and an anonymous reviewer for their detailed and constructive
177 revisions. This work was partly funded by FIRB-MIUR Project “Development of innovative
178 technologies for the environmental protection from natural events”.

179 **REFERENCES CITED**

- 180 Andronico, D., Cristaldi, A., Del Carlo, P., and Taddeucci, J., 2009, Shifting styles of basaltic
181 explosive activity during the 2002–03 eruption of Mt. Etna, Italy: Journal of Volcanology and
182 Geothermal Research, v. 180, p. 110–122, doi: 10.1016/j.jvolgeores.2008.07.026.
- 183 Arrighi, S., Principe, C., and Rosi, M., 2001, Violent Strombolian and Subplinian eruptions at
184 Vesuvius during post-1631 activity: Bulletin of Volcanology, v. 63, p. 126–150, doi:
185 10.1007/s004450100130.
- 186 Di Traglia, F., Cimarelli, C., De Rita, D., and Gimeno Torrente, D., 2009, Changing eruptive styles
187 in basaltic explosive volcanism: Examples from Croscat complex scoria cone, Garrotxa
188 Volcanic Field (NE Iberian Peninsula): Journal of Volcanology and Geothermal Research,
189 v. 180, p. 89–109, doi: 10.1016/j.jvolgeores.2008.10.020.
- 190 Guérin, G., Behamoun, G., and Mallarach, J.M., 1985, Un exemple de fusió parcial en medi
191 continental. El vulcanisme quaternari de la Garrotxa: Vitrina - Museu Comarcal de la Garrotxa,
192 v. 1, p 19–26.
- 193 Hill, B.E., Connor, C.B., Jarzemba, M.S., La Femina, P.C., Navarro, M., and Strauch, W., 1998,
194 1995 eruptions of Cerro Negro Volcano, Nicaragua, and risk assessment for future eruptions:
195 Geological Society of America Bulletin, v. 110, p. 1231–1241, doi: 10.1130/0016-
196 7606(1998)110<1231:EOCNVN>2.3.CO;2.
- 197 Houghton, B.F., Bonadonna, C., Gregg, C.E., Johnston, D.M., Cousins, W.J., Cole, J.W., and Del
198 Carlo, P., 2006, Proximal tephra hazards: recent eruption studies applied to volcanic risk in the
199 Auckland volcanic field, New Zealand: Journal of Volcanology and Geothermal Research,
200 v. 155, no. 1–2, p. 138–149, doi: 10.1016/j.jvolgeores.2006.02.006.
- 201 Houghton, B.F., and Gonnermann, H.M., 2008, Basaltic explosive volcanism: Constraints from
202 deposits and models: Chemie der Erde - Geochemistry, v. 68 (2), p. 117–140.
- 203 Keating, G.N., Valentine, G.V., Krier, D.J., and Perry, F.V., 2008, Shallow plumbing systems for
204 small-volume basaltic volcanoes: Bulletin of Volcanology, v. 70, p. 563–582, doi:
205 10.1007/s00445-007-0154-1.

- 206 Lautze, N.C., and Houghton, B.F., 2007, Linking variable explosion style and magma textures
207 during 2002 at Stromboli volcano, Italy: *Bulletin of Volcanology*, v. 69, p. 445–460, doi:
208 10.1007/s00445-006-0086-1.
- 209 Lautze, N.C., and Houghton, B.F., 2005, Physical mingling of magma and complex eruption
210 dynamics in the shallow conduit at Stromboli volcano, Italy: *Geology*, v. 33, no. 5, p. 425–428,
211 doi: 10.1130/G21325.1.
- 212 Lejeune, A.M., and Richet, P., 1995, Rheology of crystal-bearing silicate melts: an experimental
213 study at high viscosities: *Journal of Geophysical Research*, v. 100, B3, p. 4215–4229, doi:
214 10.1029/94JB02985.
- 215 Luhr, J.F., and Simkin, T., 1993, Paricutín: The Volcano Born in a Mexican Cornfield: *Geoscience*
216 Press Inc., Phoenix, Arizona, 427 p.
- 217 MacDonald, G.A., 1972, *Volcanoes*: Prentice-Hall Inc., Englewood Cliffs, New Jersey. 510 p.
- 218 Mangan, M.T., and Cashman, K.V., 1996, The structure of basaltic scoria and reticulite and
219 inferences for vesiculation, foam formation, and fragmentation in lava fountains: *Journal of*
220 *Volcanology and Geothermal Research*, v. 73, p. 1–18, doi: 10.1016/0377-0273(96)00018-2.
- 221 Parfitt, E.A., 2004, A discussion of the mechanisms of explosive basaltic eruptions: *Journal of*
222 *Volcanology and Geothermal Research*, v. 134, no. 1–2, p. 77–107, doi:
223 10.1016/j.jvolgeores.2004.01.002.
- 224 Pioli, L., Erlund, E., Johnson, E., Cashman, K., Wallace, P., Rosi, M., and Delgado Granados, H.,
225 2008, Explosive dynamics of violent Strombolian eruptions: The eruption of Parícutin Volcano
226 1943–1952 (Mexico): *Earth and Planetary Science Letters*, v. 271, p. 359–368, doi:
227 10.1016/j.epsl.2008.04.026.
- 228 Pioli, L., Azzopardi, B.J., and Cashman, K.V., 2009, Controls on the explosivity of scoria cone
229 eruptions: Magma segregation at conduit junctions: *Journal of Volcanology and Geothermal*
230 *Research*, v. 186, p. 407–415, doi: 10.1016/j.jvolgeores.2009.07.014.

- 231 Polacci, M., Baker, D.R., Bai, L., and Mancini, L., 2008, Large vesicles record pathways of
232 degassing at basaltic volcanoes: *Bulletin of Volcanology*, v. 70, no. 9, p. 1023–1029, doi:
233 10.1007/s00445-007-0184-8.
- 234 Rosi, M., Bertagnini, A., Harris, A.J.L., Pioli, L., Pistolesi, M., and Ripepe, M., 2006, A case
235 history of paroxysmal explosion at Stromboli: Timing and dynamics of the April 5, 2003 event:
236 *Earth and Planetary Science Letters*, v. 243, p. 594–606, doi: 10.1016/j.epsl.2006.01.035.
- 237 Sable, J.E., Houghton, B.F., Del Carlo, P., and Coltelli, M., 2006, Changing conditions of magma
238 ascent and fragmentation during the Etna 122 BC basaltic Plinian eruption: Evidence from clast
239 microtextures: *Journal of Volcanology and Geothermal Research*, v. 158, p. 333–354, doi:
240 10.1016/j.jvolgeores.2006.07.006.
- 241 Taddeucci, J., Pompilio, M., and Scarlato, P., 2002, Monitoring the explosive activity of the July-
242 August 2001 eruption of Mt. Etna (Italy) by ash characterization: *Geophysical Research
243 Letters*, v. 29, p. X1–X4, doi: 10.1029/2001GL014372.
- 244 Taddeucci, J., Pompilio, M., and Scarlato, P., 2004, Conduit processes during the July-August 2001
245 explosive activity of Mt. Etna (Italy): inferences from glass chemistry and crystal size
246 distribution of ash particles: *Journal of Volcanology and Geothermal Research*, v. 137, p. 33–
247 54, doi: 10.1016/j.jvolgeores.2004.05.011.
- 248 Taddeucci, J., Scarlato, P., Andronico, D., Cristaldi, A., Zimanowski, B., Büttner, R., and Küppers,
249 U., 2007, Advances in the study of volcanic ash: *Eos, Transactions, American Geophysical
250 Union*, v. 88, no. 24, p. 253–260, doi: 10.1029/2007EO240001.
- 251 Toramaru, A., 2006, BND (Bubble-Number Density) decompression rate meter for explosive
252 volcanic eruptions: *Journal of Volcanology and Geothermal Research*, v. 154, p. 303–316, doi:
253 10.1016/j.jvolgeores.2006.03.027.
- 254 Valentine, G.A., Krier, D., Perry, F.V., and Heiken, G., 2005, Scoria cone construction
255 mechanisms, Lathrop Wells volcano, southern Nevada, USA: *Geology*, v. 33, p. 629–632, doi:
256 10.1130/G21459.1.

257 Valentine, G.A., Krier, D.J., Perry, F.V., Heiken, G. 2007, Eruptive and geomorphic processes at
258 Lathrop Wells scoria cone volcano. *Journal of Volcanology and Geothermal Research*, v. 161,
259 p. 57–80, doi:10.1016/j.jvolgeores.2006.11.003

260 Valentine, G.A., and Gregg, T.K.P., 2008, Continental basaltic volcanoes - Processes and problems:
261 *Journal of Volcanology and Geothermal Research*, v. 177, p. 857–873, doi:
262 10.1016/j.jvolgeores.2008.01.050.

263 Vergniolle, S., and Mangan, M., 2000, Hawaiian and Strombolian eruptions, in Sigurdsson, H.,
264 Houghton, B., McNutt, S., Rymer, H., Stix, J. eds., *Encyclopedia of Volcanoes*. Academic
265 Press, San Diego, CA, pp. 447–461.

266 FIGURE CAPTIONS

267 Figure 1. Location (a), integrated stratigraphy and sampled levels (b), and square root of area versus
268 thickness plot for violent Strombolian deposits of the CCSC, also showing the fields of violent
269 Strombolian and Subplinian deposits (after Arrighi et al. 2001) (c).

270 Figure 2. a) Dark-gray, tachylite-like microlite-rich domains (MRD) and light-gray, sideromelane-
271 like microlite-poor (MPD) ones in mingled scoriae of the CCSC (polarized light). b, c) BSE image
272 of the two domains. Note microlite-rich MRD groundmass (darker gray, silica-enriched interstitial
273 glass) and MPD (lighter gray, silica-poor glass with higher vesicularity). Microlites are black,
274 elongated Plg, gray, zoned Cpx, light gray Ol, and white Ox. d, e, f) fluidal morphologies of MRD
275 (white outlines) with Ol phenocrysts (dark gray) occurring in both domains. g) CaO versus MgO
276 plot of the interstitial glass (MPD and MRD) and bulk (MRD only) compositions from all samples
277 (in the inset, an example of FE-SEM spot and raster areas for the chemical analysis of interstitial
278 glass and bulk composition, respectively).

279 Figure 3. Relative abundance (vol.%; $\pm 1\sigma$ error bar) of MP clasts up-section in the Croscat
280 deposits. Eruption duration is estimated to be several months. Dashed line (third order polynomial
281 best fit) highlights the sharp increase in the MP clasts abundance in the UQU Strombolian deposits
282 anticipating the CMU violent Strombolian ones.

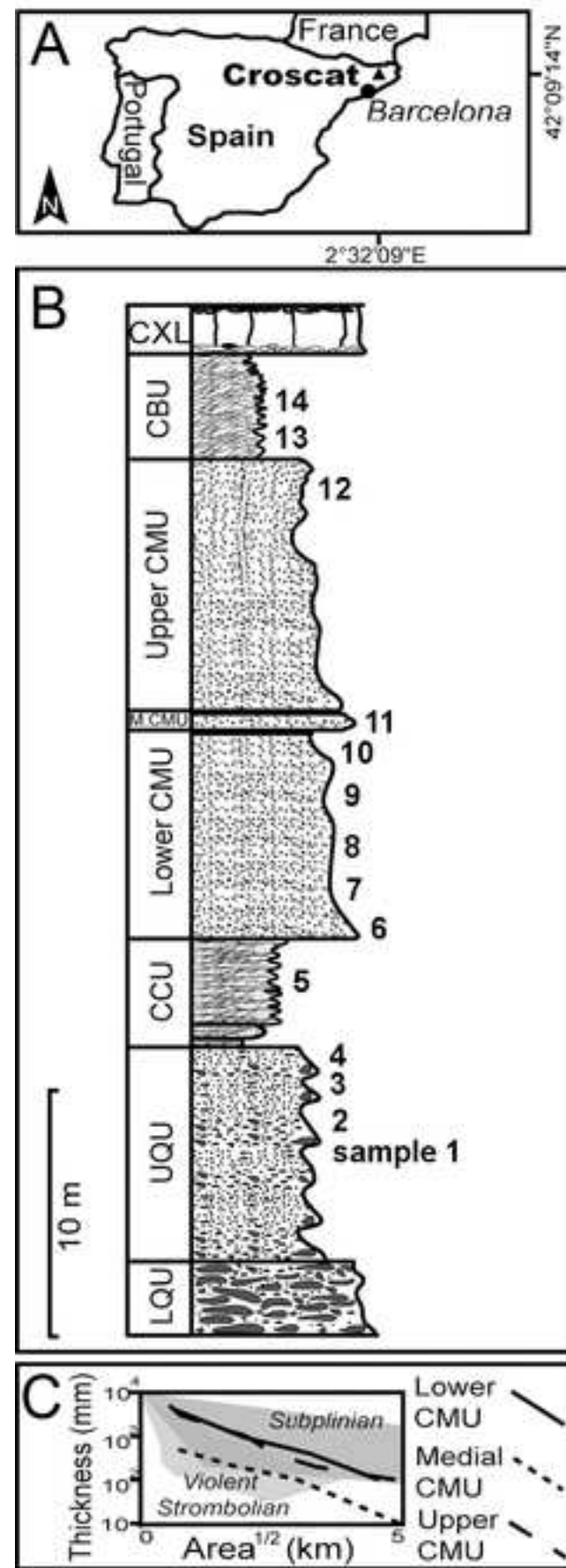
283 Figure 4. Interpretative scheme of the Croscat eruptive conduit. a) Mingling interface between the
284 MR and MP magmas (conduit margin and central flow line are toward the left and right hand sides
285 of the figure, respectively). Grey arrows represent flow velocity. b) During the Strombolian phase,
286 magma flow velocity is relatively low and the MR zone is well developed. c) The buoyant lift from
287 the underlying, volatile-rich magma increases flow velocity and reduces the MR zone. d) Flow
288 velocity escalates as volatile-rich magma vesiculates and the more viscous, volatile-poor magma is
289 evacuated. e) Flow velocity decreases after the first arrival of the gas-charged magma and the onset
290 of violent Strombolian activity. Similar ascent velocities in c) and e) result in very different activity
291 at the vent due to the different volatile content of the erupting magma.

292 ¹GSA Data Repository item 2009xxx, xxxxxxxx, is available online at
293 www.geosociety.org/pubs/ft2008.htm, or on request from editing@geosociety.org or Documents
294 Secretary, GSA, P.O. Box 9140, Boulder, CO 80301, USA.

Figure_1

[Click here to download high resolution image](#)

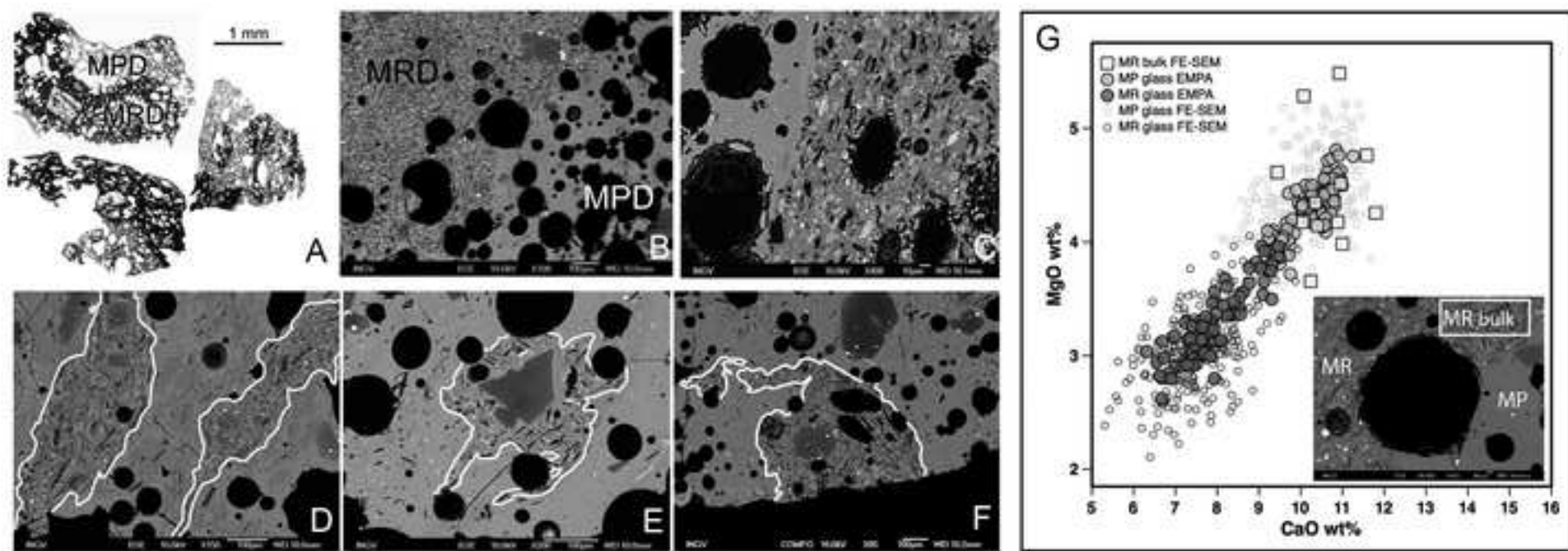
Cimarelli et al., Fig. 1, TIFF



Figure_2

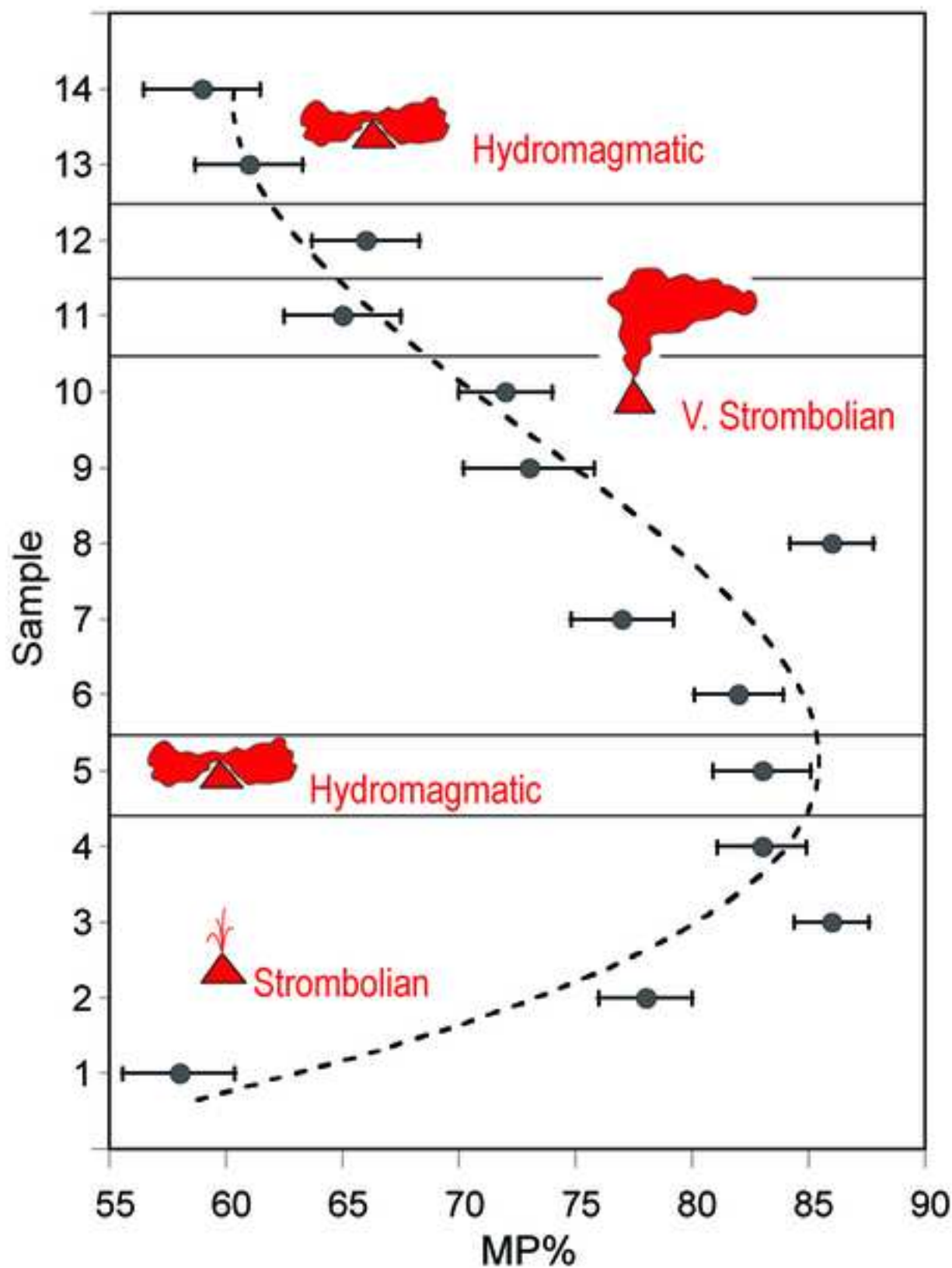
[Click here to download high resolution image](#)

Cimarelli et al., Fig. 2, TIFF



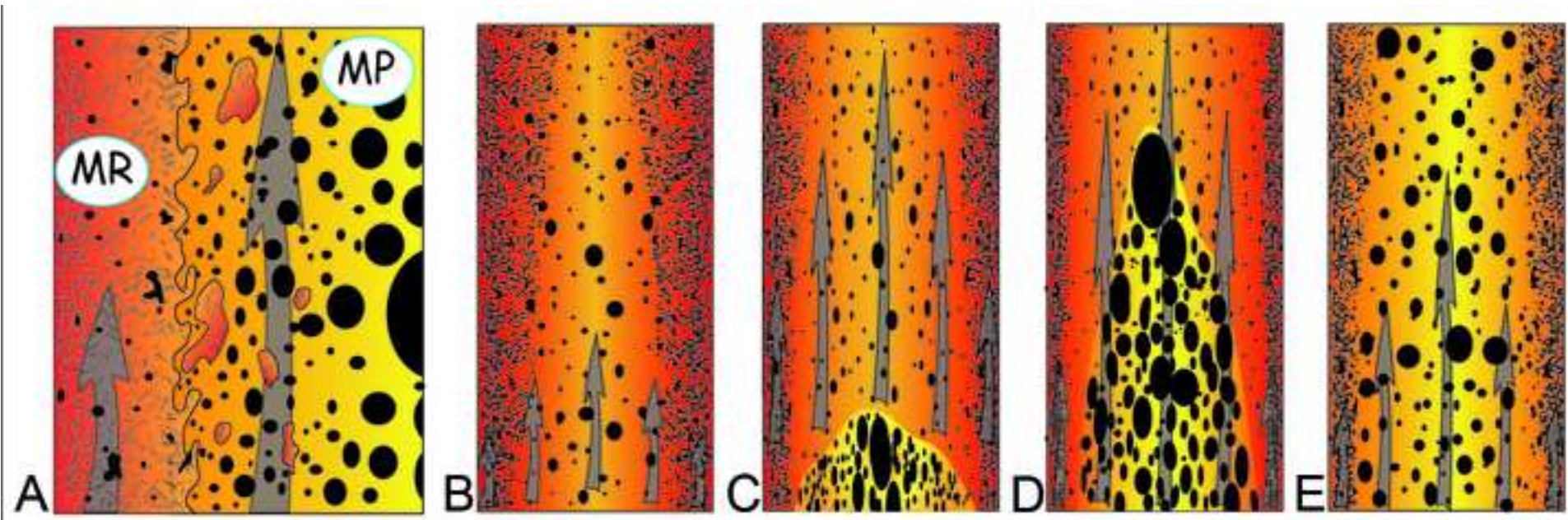
Figure_3
[Click here to download high resolution image](#)

Cimarelli et al., Fig. 3, TIFF



Figure_4

[Click here to download high resolution image](#)



Cimarelli et al., Fig. 4, TIFF